

Weak Acid Permeability through Lipid Bilayer Membranes

Role of Chemical Reactions in the Unstirred Layer

ANNE WALTER, DAVID HASTINGS, and JOHN GUTKNECHT

From the Department of Physiology, Duke University Medical Center, Durham, North Carolina 27710; the Duke University Marine Laboratory, Beaufort, North Carolina 28516; and the Division of Biochemistry, Physiology and Pharmacology, University of South Dakota, School of Medicine, Vermillion, South Dakota 57069

ABSTRACT The permeabilities of planar lipid bilayer (egg phosphatidylcholine-decane) membranes to butyric and formic acids were measured by tracer and pH electrode techniques. The purposes of the study were (a) to establish criteria for the applicability of each method and (b) to resolve a discrepancy between previously published permeabilities determined using the different techniques. Tracer fluxes of butyric acid were measured at several concentrations and pH's. Under symmetrical conditions the one-way flux of butyric acid (J) is described by $1/J = 1/P^{ul} ([HA] + [A^-]) + 1/P^m([HA])$, where P^{ul} and P^m are the unstirred layer and membrane permeability coefficients. P^m determined in this manner is $950 \times 10^{-4} \text{ cm s}^{-1}$. Published values for the butyric acid permeability for egg phosphatidylcholine-decane bilayers are 11.5×10^{-4} (Wolosin and Ginsburg, 1975) and $640 \times 10^{-4} \text{ cm s}^{-1}$ (Orbach and Finkelstein, 1980). Wolosin and Ginsburg measured net fluxes from a solution of $\text{pH} = \text{p}K_a$ into an unbuffered solution containing a pH electrode. Orbach and Finkelstein measured tracer fluxes under symmetrical conditions at pH 7.4. We reproduced the results of Wolosin and Ginsburg and showed that their apparently low P^m was caused by unstirred layer effects in their poorly buffered solutions. The permeability to formic acid ($\text{p}K_a = 3.75$) measured by both tracer and pH electrode techniques was $\sim 10^{-2} \text{ cm s}^{-1}$. However, if $P^m > P^{ul}$, the pH electrode technique cannot be used for measuring the permeabilities of weak acids with $\text{p}K_a$'s greater than ~ 4 .

INTRODUCTION

Some important biological molecules, e.g., many nutrients, metabolites, and drugs, are weak acids or bases. Weak acids are also among the useful nonelectrolyte probes of lipid bilayer structure. Thus it is important to

Address reprint requests to Dr. Anne Walter, Laboratory of Kidney and Electrolyte Metabolism, Building 10, Room 6N307, National Heart, Lung, and Blood Institute, National Institutes of Health, Bethesda, MD 20205.

J. GEN. PHYSIOL. © The Rockefeller University Press • 0022-1295/82/05/0917/17\$1.00 917

Volume 79 May 1982 917-933

establish proper methods for measuring weak acid permeability coefficients across biological and model membrane systems. Two laboratories that have been characterizing the physical nature of the bilayer using nonelectrolyte permeability patterns draw conflicting conclusions regarding the structure of the lipid bilayer, and they report very different values for the permeability of butyric acid (the only permeability they both measured) across egg phosphatidylcholine-decane bilayers. Orbach and Finkelstein (1980) measured one-way tracer fluxes under symmetrical conditions at pH 7.4 (i.e., $\text{pH} \gg \text{p}K_a$ of butyric acid) and report a permeability of $640 \times 10^{-4} \text{ cm s}^{-1}$. Wołosin and Ginsburg (1975) used a pH electrode to measure net fluxes from a solution at a pH equal to the $\text{p}K_a$ of the acid into an unbuffered solution at pH ~ 8.5 . They corrected for unstirred layer effects using an independent measurement of the unstirred layer thickness and obtained a membrane permeability of $11.5 \times 10^{-4} \text{ cm s}^{-1}$.

We hypothesized that the difference in the reported permeabilities could be attributed to the different methods used for flux measurements. In this study we compared the two methods and established conditions under which each can be used. First, it is necessary to understand how the associated and dissociated forms of a weak acid interact in the unstirred layer under different conditions. Then these interactions can be used by the investigator to determine actual membrane permeability coefficients.

The nonionic forms of many weak acids are sufficiently nonpolar so that according to Overton's rule the membrane permeabilities of these molecules are expected to be high. In many cases, the permeabilities are so high ($>10^{-3} \text{ cm s}^{-1}$) that diffusion through the aqueous unstirred layers adjacent to the membrane is the rate-limiting step for diffusion across the membrane system, and the true membrane permeability cannot be determined from simple flux measurements. Furthermore, weak acids exist in both nonionic (HA) and ionic (A^-) forms so that membrane permeability estimates are complicated by gradients in pH and A^- , as well as HA, across the unstirred layers. However, any solute that exists in both a permeant (nonionic) and impermeant (ionic) form can undergo "facilitated" diffusion through the unstirred layer because of reactions between the two forms. In other words, the gradient in the total acid concentration through the unstirred layer is composed of the gradients of HA and A^- , even though only HA permeates the membrane. A^- reacts with H^+ in the unstirred layer, providing additional HA at the membrane surface and thus increasing the flux of HA through the membrane. Under symmetrical or highly buffered conditions, when pH is constant through the unstirred layer, we can express the complex flux relationship as follows (Gutknecht and Tosteson, 1973):

$$\frac{1}{J} = \frac{1}{P_{\text{HA}}^{\text{ul}}[\text{HA}] + P_{\text{A}^-}^{\text{ul}}[\text{A}^-]} + \frac{1}{P_{\text{HA}}^{\text{m}}[\text{HA}]} \quad (1)$$

where J is the flux, and P^{ul} and P^{m} are the unstirred layer and membrane permeability coefficients. If the relative concentrations of the two forms are adjusted such that $[\text{A}^-] \gg [\text{HA}]$, virtually all of the gradient in total acid through the unstirred layer is represented by A^- . Under these conditions the

unstirred layer term in Eq. 1 is small compared with the membrane term, and the relationship approaches $1/J = 1/(P_{HA}^m [HA])$ and the actual membrane permeability to HA can then be determined directly from flux measurements. A similar approach can be used to measure membrane permeabilities to weak bases (Gutknecht and Walter, 1981c).

Eq. 1 can be simplified by assuming that $P_{HA}^{ul} = P_{A^-}^{ul}$, which is valid because the difference in the aqueous diffusion coefficients of the two species will generally be on the order of a few percent (Robinson and Stokes, 1959), much less than the other errors in the permeability measurements. This allows us to convert Eq. 1 to two linear equations with the membrane and unstirred layer permeabilities as the reciprocals of the slopes, i.e.,

$$\frac{[A_T]}{J} = \frac{1}{P^m} \frac{[A_T]}{[HA]} + \frac{1}{P^{ul}}; \quad (2)$$

$$\frac{[HA]}{J} = \frac{1}{P^{ul}} \frac{[HA]}{[A_T]} + \frac{1}{P^m} \quad (3)$$

where $[A_T] = [HA] + [A^-]$. These two equations are useful because flux data from different A_T concentrations and pH's can be combined and statistical estimates of the permeabilities can be obtained. Second, data from conditions under which the membrane is not entirely rate limiting can be used to estimate the true membrane permeability, which is important in practice, as occasionally it is not possible to form membranes under the conditions required for the observed flux to be limited solely by the membrane.

Net fluxes of acids measured with a pH electrode can also be used to estimate membrane permeabilities if the unstirred layer effects can be minimized. This can be achieved by ensuring that (a) the total permeability of the *cis* unstirred layer is high ($[A^-] \gg [HA]$, well-buffered solution) and (b) the back flux is much smaller than the forward flux (*trans* pH $>$ p*K*_a or $P^m < P^{ul}$). The transmembrane gradient in HA can then be calculated (see Appendix) and the membrane permeability can be obtained from the relation,

$$P_{HA}^m = \frac{J_{H^+}^{net}}{[HA]^{cis} - [HA]^{trans}}. \quad (4)$$

In this study we established the validity of Eqs. 1–3 by measuring tracer fluxes of butyric acid over a wide range of pH. We also measured the membrane permeability to formic acid by both tracer and pH electrode techniques in order to show consistency between the two methods and to demonstrate the validity of the iterative solution for $[HA]^{trans}$ as required for Eq. 4.

MATERIALS AND METHODS

General

Lipid bilayer membranes were made by the brush technique of Mueller and Rudin (1969) from a solution of egg phosphatidylcholine in decane (28–30 mg/ml). Membranes were formed on a 1.6-mm² hole in a polyethylene partition separating two magnetically stirred, 1.25-ml chambers. Ag/AgCl or calomel electrodes were placed

on either side of the membrane and membrane resistances were calculated from current/voltage curves.

Egg phosphatidylcholine (Lipid Products, Surrey, England) migrated as a single spot on a thin-layer chromatography plate. All buffers and decane were from Sigma Chemical Co. (St. Louis, MO). The decane was passed through an alumina column before use. ^{14}C -butanol (New England Nuclear Boston, MA), ^{14}C -butyric acid, ^{14}C -formic acid, and ^{14}C -salicylic acid (International Chemical and Nuclear Corporation Irvine, CA) were used as purchased. The butyric acid had no radiochemical impurities that were more lipophilic than itself as determined by repeated extractions into decane or hexadecane.

Tracer Experiments

Unless otherwise specified, the membranes were bathed with symmetrical weak acid solutions. Ionic strength was generally held constant at either 0.1 or 0.2 with NaCl that had been roasted for 12 h at 500°C . All solutions contained 5 or 10 mM buffer: citrate (pH 3.7 and 4.7), MES (pH 5.7), PIPES (pH 6.7), HEPES (pH 7.2 and 7.7), TRICINE (pH 8.2). Total acid concentrations varied and were determined at constant acid (HA) or anion (A^-) concentrations by the Henderson-Hasselbalch equation:

$$\text{pH} = \text{p}K_a + \log \frac{[\text{A}^-]}{[\text{HA}]} \quad (5)$$

The $\text{p}K_a$ for butyric acid at infinite dilution is 4.84, but when corrected for ionic strengths of 0.1–0.2, the $\text{p}K_a$ is ~ 4.7 (Perrin and Dempsey, 1974). Similarly, the $\text{p}K_a$ for formic acid is 3.75, but when corrected for ionic strength effects, it is 3.64. The temperature was $22 \pm 2^\circ\text{C}$.

As soon as the membranes were optically black, 0.7–5.0 μCi of ^{14}C -labeled acid was injected into the *cis* chamber. The *trans* chamber was perfused continuously at 0.5–1.5 ml/min. The perfusate was collected in a vacuum trap at 3-min intervals for ~ 30 min. The flux generally reached steady state between 6 and 9 min after injection of tracer. The *cis* chamber was sampled periodically. Samples were mixed with Aquasol or Aquasol II scintillation cocktail (New England Nuclear) and counted in a liquid scintillation counter (LS 100; Beckman Instruments, Inc., Fullerton, CA). Counts were converted to disintegrations per minute (dpm) using the external standard ratio. Fluxes were determined using the equation:

$$J = \frac{{}^{14}\text{C}^{\text{trans}}}{t A sa^{\text{cis}}} \quad (6)$$

where J is the flux in $\text{mol cm}^{-2} \text{s}^{-1}$, ${}^{14}\text{C}^{\text{trans}}$ is the total amount of tracer (μCi) entering the front compartment during the time interval t (s), A is the membrane surface area (cm^2), and sa^{cis} is the specific activity of labeled acid in the rear compartment ($\mu\text{Ci mol}^{-1}$).

The unstirred layer thickness was determined from the ^{14}C -butanol flux (Holz and Finkelstein, 1970). The membrane permeability to butanol is predicted by its ether/water partition coefficient to be so high that the flux will be totally limited by the unstirred layer permeability. The thickness of the unstirred layer was calculated from the relationship:

$$\delta^{\text{ul}} = \frac{D}{P^{\text{ul}}} \quad (7)$$

where δ^{ul} is the unstirred layer thickness, D is the butanol aqueous diffusion coefficient, and P^{ul} is the butanol unstirred layer permeability coefficient. The aqueous diffusion

coefficient for butanol is $1 \times 10^{-5} \text{ cm}^2 \text{ s}^{-1}$ (Lyons and Sandquist, 1953) and the measured butanol permeability is $(4.15 \pm 1.75) \times 10^{-4} \text{ cm s}^{-1}$.

pH Electrode Experiments

Net fluxes of formic acid were measured by using a pH electrode and observing the rate of change in pH of the *trans* solution. The *cis* solution was perfused continuously with Na formate (20 mM) and MES (30 mM) at pH 5.9, and the *trans* solution contained unbuffered NaCl (50 mM) with pH ranging from 5.7 to 6.5. All solutions were equilibrated with argon, and an argon atmosphere was maintained above the solutions to minimize the absorption of CO_2 . The $\text{p}K_a$ of formic acid at ionic strength of 0.05 is 3.66.

The unstirred layer thickness in the electrode-containing solution was determined separately because the presence of the pH electrode slightly reduced the efficiency of stirring. ^{14}C -salicylic acid (0.1 mM) was added to the electrode-containing solution, which was unbuffered NaCl (50 mM, titrated to pH 3.0 with HCl). The opposite side contained Na HEPES (50 mM, pH 7.6). The membrane permeability to salicylic acid is sufficiently high (ca. 0.8 cm s^{-1}) (Gutknecht and Tosteson, 1973) that the net flux is limited solely by the unstirred layer permeability in the electrode-containing solution. Furthermore, salicylic acid permeability is at least 10^5 times higher than salicylate permeability, so the assumptions of Eq. 1 are valid.

P^m in these experiments was calculated by assuming virtually no unstirred layer effect in the well-buffered *cis* solution and using the value of $[\text{HA}]_{\text{trans}}^m$ calculated as outlined in the Appendix. Aqueous diffusion coefficients were calculated from the limiting equivalent conductivities of the ions, λ° , and the Nernst relation, $D^\circ = \lambda^\circ (RT/zF^2)$ (Robinson and Stokes, 1959).

RESULTS

Acid Is the Primary Species Crossing the Membrane

The maximum flux of A^- can be calculated from the membrane resistance and the relationship (Hodgkin, 1951):

$$J_{\text{A}^-} = \frac{RT}{z^2 F^2} G_{\text{A}^-} \quad (8)$$

where J_{A^-} is the predicted flux of butyrate, R is the gas constant, F is the Faraday, z is the valence of the anion, and G_{A^-} is the butyrate conductance. The total membrane conductances for all experiments ranged from 20 to 2,000 nS cm^{-2} and are in the normal range for egg phosphatidylcholine-decane membranes. If the entire conductance of the most conductive membrane was caused by butyrate flux, the A^- flux would be $5.3 \times 10^{-13} \text{ mol cm}^{-2} \text{ s}^{-1}$. Because the minimum tracer flux observed was $2.7 \times 10^{-11} \text{ mol cm}^{-2} \text{ s}^{-1}$, A^- could account for a maximum of 2% of the total flux. All fluxes were two to five orders of magnitude greater than the calculated maximum A^- flux. Thus, the assumption that only HA crosses the membrane (required for the derivation of Eq. 1) is valid for butyric acid.

HA and A^- Dependence of the One-Way Tracer Flux

The model described by Eq. 1 predicts that when $P^{\text{ul}} [\text{A}_T] \gg P^m [\text{HA}]$, the flux will be determined by the membrane permeability, whereas when P^{ul}

$[A_T] \ll P^m[HA]$, the unstirred layer permeability will limit the flux. The relative values of these parameters can easily be varied at constant $[HA]$ or $[A^-]$ by adjusting the pH and varying the total acid concentration. We used both of these approaches in order to describe the different rate-limiting steps under different conditions (Figs. 1 and 2). In Fig. 1 the flux is plotted against $[HA]$ at constant $[A^-]$ (10^{-3} M). At high pH (7.2–8.2), the value of $1/P^{ul}[A_T]$ is fairly constant and small relative to $1/P^m[HA]$, so that the linear increase in flux over this region represents a membrane-limited flux. Over the

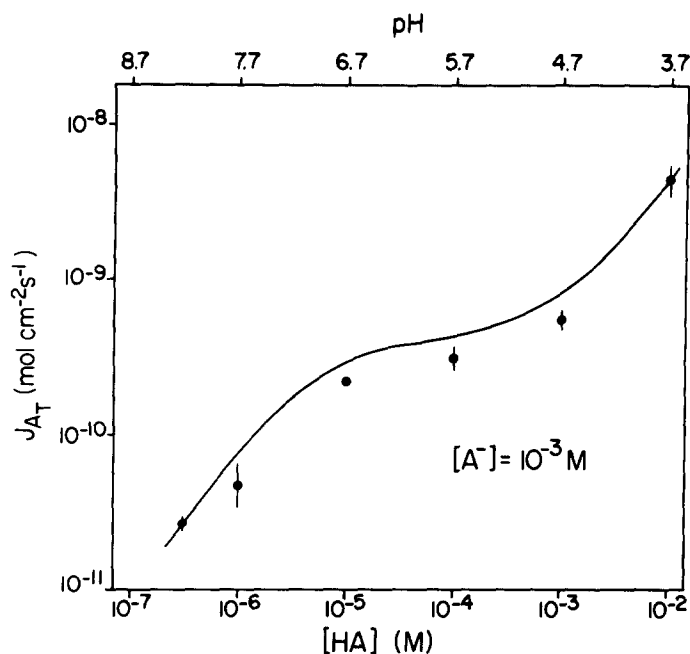


FIGURE 1. The one-way flux of butyric acid as a function of the concentration of the nonionic form (HA) at a constant concentration of the ionic form (A^-). The front and rear solutions are identical except for the addition of ^{14}C -butyrate to the rear compartments and are buffered as outlined in Materials and Methods. Each point is the mean of measurements on three membranes and the vertical bars are the standard deviations. The smooth curve is calculated from Eq. 1, using $P^m = 9.5 \times 10^{-2}$ cm s⁻¹ and $P^{ul} = 4.2 \times 10^{-4}$ cm s⁻¹.

central flat portion of the curve, $1/P^{ul}[A_T]$ is nearly constant and large relative to $1/P^m[HA]$; thus the flux is constant and determined by the unstirred layer term. At $pH \leq 4.7$, $[A_T]$ increases and the total flux across the unstirred layer and membrane increases linearly with $[HA]$ with the unstirred layer term being rate limiting.

A similar analysis can be made in Fig. 2, where the flux is plotted against the ratio of $[A^-]$ to $[HA]$ at constant $[HA]$. At low pH the flux is independent of $[A^-]$ and is rate-limited by diffusion of HA across the unstirred layer. As the pH increases, the relative proportion of HA decreases and the term

$1/P^{ul}[A_T]$ increases so that the resistance of the unstirred layer is decreasing relative to that of the membrane but still larger than the membrane resistance. At high pH the flux is again independent of $[A^-]$ because $1/P^{ul}[A_T]$ is small relative to $1/P^m[HA]$.

The points in Figs. 1 and 2 are the means of experimental observations and the smooth curves were drawn from Eq. 1 using values of P^m and P^{ul} calculated by Eqs. 2 and 3. All data were pooled to determine values of P^m and P^{ul} from Eqs. 2 and 3 with P^m being 9.5×10^{-2} [(9.0–10.1) $\times 10^{-2}$] cm s^{-1} and P^{ul} being 4.2×10^{-4} [(4.0–4.3) $\times 10^{-4}$] cm s^{-1} (range predicted by

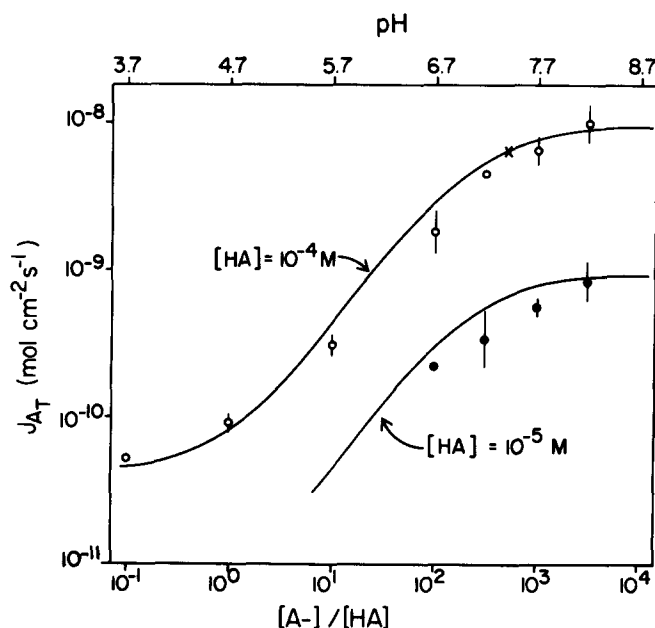


FIGURE 2. The one-way flux of butyric acid as a function of the ratio of $[A^-]$ to $[HA]$ at constant $[HA]$ (open circles, $[HA] = 10^{-4}$ M; closed circles, $[HA] = 10^{-5}$ M). The *cis* and *trans* solutions are identical except for addition of tracer to the *cis* compartment. Points are means of three membranes and the vertical bars are the standard deviations. The smooth curves are calculated from Eq. 1 using $P^m = 9.5 \times 10^{-2}$ cm s^{-1} and $P^{ul} = 4.2 \times 10^{-4}$ cm s^{-1} .

standard deviation of the slope). The slopes from the least-squares linear regression were used to estimate the permeabilities because these are more accurately predicted than the intercepts. However, the values of P^{ul} and P^m predicted by the intercepts are similar to those determined by the slopes. The data in Fig. 2 at $[HA] = 10^{-4}$ M and $[HA] = 10^{-5}$ M were compared using Eq. 2 to see if the permeability coefficient was affected by the absolute concentrations of HA or A^- . The regression lines were indistinguishable, which indicates that neither P^m nor P^{ul} was altered by the 10-fold difference in $[HA]$ and $[A^-]$.

The unstirred layer thickness calculated from the butyric acid unstirred

layer permeability coefficient and the aqueous diffusion coefficient, $8.67 \times 10^{-6} \text{ cm}^2 \text{ s}^{-1}$, estimated from the Nernst limiting conductance of butyrate and the ionic strength (Robinson and Stokes, 1959), is $206 \pm 9 \mu\text{m}$. This is similar to the value estimated from the butanol flux, i.e., $241 \pm 176 \mu\text{m}$, which confirms that the model described by Eq. 1 gives an accurate estimate of P^{ul} .

Further indication that the flux across the membrane is due to HA and is independent of A^- at high pH is seen in Fig. 3, which is a plot of the flux vs. $[\text{HA}]$ at pH 8.2 and pH 7.7. The fluxes at pH 7.7 are slightly lower than those at pH 8.2 because of a small effect of the unstirred layer at pH 7.7 (see Fig. 2). However, the differences between fluxes for the same HA concentration at these pH's are far less than the 3.2-fold difference in $[\text{A}^-]$ at all points. The

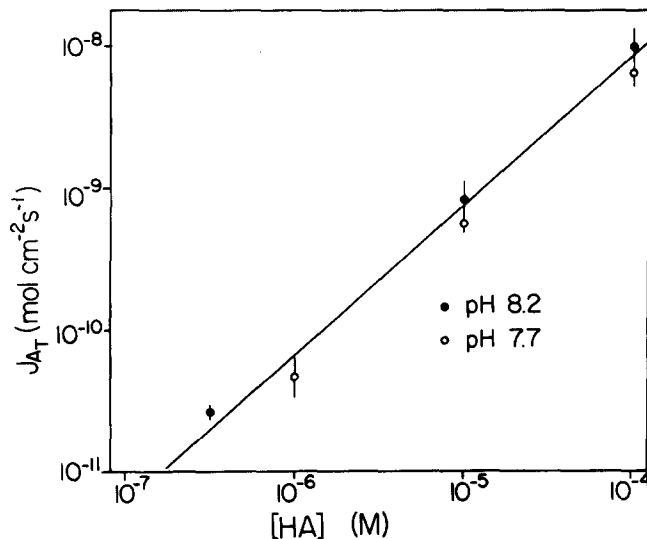


FIGURE 3. Butyric acid flux as a function of $[\text{HA}]$ at pH 7.7 (open circles) and pH 8.2 (closed circles). The points are means from three membranes and the vertical bars are the standard deviations. The line is the least-squares fit to the data and has a slope of 1.0.

slope of the regression line is 1.0, which indicates a direct proportionality between the flux and $[\text{HA}]$.

Role of H^+ Gradients in the Unstirred Layers

The interconversion of butyrate and butyric acid requires hydrogen ions. Hydrogen ion gradients do not exist in symmetrical experiments, because for every labeled HA that crosses the membrane from the *cis* side an unlabeled HA crosses from the *trans* side. However, in a net flux experiment at low buffer concentration, the transfer of HA across the membrane will cause a depletion of H^+ in the unstirred layer on the *cis* side of the membrane and an enrichment of H^+ in the *trans* unstirred layer. This will have two effects: (a) the pH adjacent to the membrane on the *cis* side will rise, which causes the ratio of $[\text{HA}]$ to $[\text{A}^-]$ to decrease below that of the bulk solution, and (b) the pH in the

trans unstirred layer will decrease because of the entry of HA. The net effect is a decrease in the HA available for permeation and an increase in backflux from the *trans* unstirred layer; thus there is a decrease in the net flux. The data in Table I confirm these predictions. At pH 7.2 when the flux of butyric acid is primarily membrane limited, the net flux in the presence of buffer (50 mM) is the same as the one-way flux (cf. Fig. 2). However, removal of buffer from the *trans* solution reduces the net flux 15-fold, which indicates an increase in [HA] in the *trans* unstirred layer and a large backflux of tracer.

A net tracer flux experiment designed to be equivalent to the pH electrode experiment of Wolosin and Ginsburg (1975) is also shown in Table I, line 3. In this case, the pH of the *cis* solution is set at the pK_a of the acid (intended by Wolosin and Ginsburg to maximize the buffering capacity of the *cis* solution), and the *trans* solution pH is set far above the pK_a in order to trap all incoming HA as the impermeant species A^- . The measured flux is $(6.3 \pm 0.6) \times 10^{-11}$ mol cm^{-2} s^{-1} ($n = 3$) and the apparent permeability calculated from

TABLE I
EFFECTS OF pH BUFFERING AND pH GRADIENTS ON BUTYRIC ACID FLUXES

<i>Cis</i> conditions			<i>Trans</i> conditions			Net flux
pH	[Buffer]	[HA]	pH	[Buffer]	[HA]	
	<i>M</i>	<i>M</i>		<i>M</i>	<i>M</i>	mol cm^{-2} s^{-1}
7.2	0.05 HEPES	10^{-5}	7.2	0.05 HEPES	0	56.0×10^{-11}
7.2	0.05 HEPES	10^{-5}	7.2	0	0	3.7×10^{-11}
4.7	0	10^{-4}	8	0	0	$(6.3 \pm 0.6) \times 10^{-11}$
						$n = 3$

Both fluxes at pH 7.2 were obtained from the same membrane by changing the composition of the *trans* solution during the experiment.

the bulk concentration of HA in the *cis* compartment is 6.3×10^{-4} cm s^{-1} , close to the value of 4.2×10^{-4} cm s^{-1} determined above for the unstirred layer permeability.

Permeability Measurements Using a pH Electrode

The formic acid permeability coefficient was determined from net H^+ fluxes monitored by a pH electrode in the *trans* compartment. An actual record of the change in the H^+ activity in the *trans* solution with time is shown in Fig. 4. The flux of H^+ is constant over the time period of the experiment and is derived from the production of formate in the *trans* solution as formic acid crosses the membrane.

The membrane and the unstirred layer gradients for a formic acid experiment are shown in Fig. 5. The small drops in [HA] and [H^+] across the *cis* unstirred layer were estimated by assuming linear gradients in A_T and the buffer. The gradients in the *trans* unstirred layer were calculated as outlined in the Appendix and, in this example, the calculated permeability is 6.85×10^{-3} cm s^{-1} . The mean value for the formic acid membrane permeability

coefficient determined in this manner is $(5.78 \pm 1.64) \times 10^{-3} \text{ cm s}^{-1}$. We then compared this value with the permeability determined by tracer flux measurements. The method was identical to that used for butyric acid. From the linear regression analysis (Eq. 2) we obtained a value of $7.32 (6.63\text{--}8.14) \times 10^{-3} \text{ cm s}^{-1}$, which is in good agreement with the value obtained by the pH electrode technique.

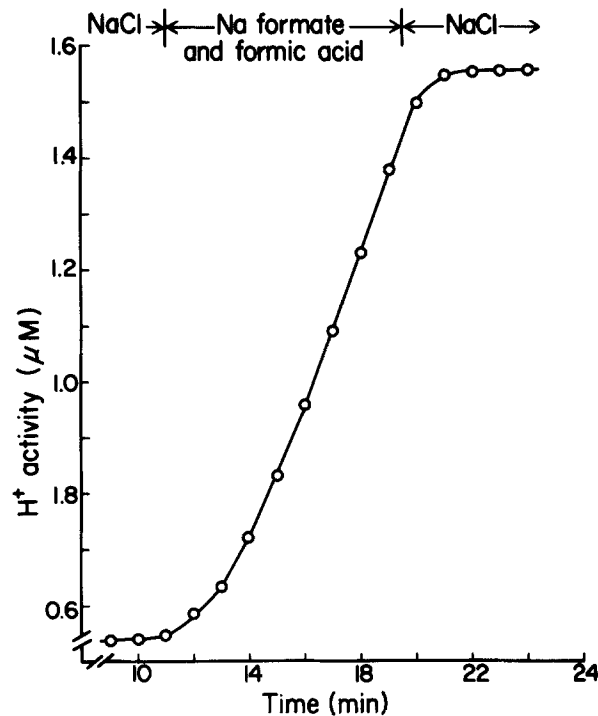


FIGURE 4. Net proton flux produced by a Na-formate and formic acid gradient across an egg phosphatidylcholine-decane lipid bilayer membrane. The H^+ activity in the *trans* solution (50 mM NaCl) was measured with a pH electrode. The *cis* solution was either NaCl (20 mM) or Na formate (20 mM). The *cis* solution also contained Na-MES buffer (30 mM, pH 5.9). The calculated formic acid concentration was $1.14 \times 10^{-4} \text{ M}$. The membrane voltage was 0 mV.

DISCUSSION

The objectives of this study were (a) to establish appropriate methods of measuring weak acid or base permeability coefficients and (b) to resolve the controversy between Orbach and Finkelstein (1980) and Wolosin and Ginsburg (1975). The tracer method involves manipulating conditions to eliminate the unstirred layer diffusion resistance. We have used tracer fluxes of butyric acid to demonstrate the validity of Eq. 1. The actual value of P^m determined from Eq. 2 ($950 \times 10^{-4} \text{ cm s}^{-1}$) is close to the $640 \times 10^{-4} \text{ cm s}^{-1}$ reported by Orbach and Finkelstein (1980), but much higher than $11.5 \times 10^{-4} \text{ cm s}^{-1}$ given by Wolosin and Ginsburg (1975). Orbach and Finkelstein used the

approach suggested by Eq. 1 when they measured the butyric acid permeability coefficient at pH 7.4 with ^{14}C -butyric acid under symmetrical conditions. There is a small and possibly insignificant difference between our value and theirs that may derive from two factors that they did not correct for or check. First, they did not consider the ionic strength effects on the $\text{p}K_a$ of weak acids. At 0.1 M salt, the $\text{p}K_a$ is depressed by ~ 0.1 pH unit (Perrin and Dempsey, 1974), and if their permeability value is corrected for this, it rises from $6.4 \times 10^{-2} \text{ cm s}^{-1}$ to $8.2 \times 10^{-2} \text{ cm s}^{-1}$. Second, they assumed that the unstirred

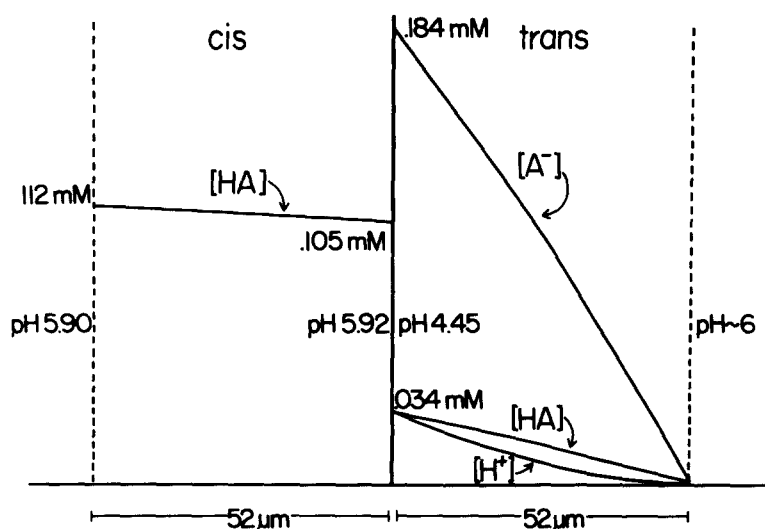


FIGURE 5. Concentration profiles in the *cis* and *trans* unstirred layers under conditions used to measure formic acid net flux using a pH electrode (see text for details). The *cis* solution contains 20 mM Na formate and 0.114 mM formic acid at pH 5.9 and 30 mM MES buffer to minimize gradients in HA through the *cis* unstirred layer. The *trans* solution is 50 mM NaCl and the gradients in [HA], [H⁺], and [A⁻] in the *trans* unstirred layer were determined as described in the Appendix. The flux is $5.11 \times 10^{-10} \text{ mol cm}^{-2} \text{ s}^{-1}$, the diffusion coefficients ($\text{cm}^2 \text{ s}^{-1}$) are $D_{\text{HA}} = 1.6 \times 10^{-5}$, $D_{\text{A}^-} = 1.45 \times 10^{-5}$, $D_{\text{H}^+} = 9.31 \times 10^{-6}$, and the activity coefficient for A⁻ and H⁺ was 0.819. Concentration gradients are drawn to scale. The unstirred layer thickness is smaller than that shown in Fig. 6 because a different bilayer chamber was used for the pH electrode experiments.

layer effects in their system would be negligible at pH 7.4. In our system, the unstirred layer term does not become insignificant until pH 8.4. Our unstirred layer thickness is somewhat larger than theirs, so the two systems are not directly comparable. However, by measuring fluxes at several pH's and calculating the permeability coefficients from the linearized equations (Eqs. 2 and 3), we have ensured that our P^m value of $9.5 \times 10^{-2} \text{ cm s}^{-1}$ is not an underestimate caused by unstirred layer effects.

In fact, the small corrections we make on Orbach and Finkelstein's butyric acid membrane permeability coefficient do not alter their general conclusions

regarding nonelectrolyte permeability through phosphatidylcholine-decane bilayers. Our value also falls on their regression line derived from the relationship $P \propto K_p D$, where P is the nonelectrolyte permeability coefficient through egg phosphatidylcholine-decane bilayers, K_p is the hexadecane/water partition coefficient, and D is the diffusion coefficient of the solute in water. From the linear relation between P and $K_p D$, they concluded that membrane permeation of nonelectrolytes is consistent with a liquid hydrocarbon model of the bilayer membrane.

The pH electrode can be used for determining the permeability of moderately strong to strong acids and bases as we have demonstrated here by the consistency between the values for the permeability coefficient of formic acid determined by tracer and net H^+ fluxes. Previous experiments from this laboratory demonstrate the usefulness of the technique when tracer fluxes are not feasible technically (Gutknecht and Walter, 1981a and b). The limiting factors are the rate of decrease in pH due to CO_2 absorption in the electrode-containing solution, the geometry of the system, and the pK_a of the permeant acid or base. This technique is feasible for weak acids with a pK_a less than (or weak bases with pK_a greater than) the pH adjacent to the *trans* side of the membrane. The pH at the *trans* membrane surface will deviate increasingly from the pH of the bulk solution as the unstirred layer thickness increases or the flux increases. Given the volume of our chamber and our unstirred layer thickness, the method is feasible for strong acids such as HCl and HNO_3 (Gutknecht and Walter, 1981a and b) formic and salicylic acid (pK_a 3.7 and 3.0, respectively), but not butyric acid (pK_a 4.7) and many other monocarboxylic acids.

The pH electrode method was used by Wolosin and Ginsbury (1975) to determine a large number of weak acid permeabilities. However, we feel that they misinterpreted their H^+ fluxes because they did not consider the interactions among A^- , H^+ , and HA in the unstirred layers. As noted above, their value for P^m of butyric acid is much lower than ours, as is the value they report for the formic acid permeability coefficient, $2.34 \times 10^{-4} \text{ cm s}^{-1}$, in contrast to our value of $\sim 8 \times 10^{-3} \text{ cm s}^{-1}$.

We used ^{14}C -butyric acid to measure fluxes under the same conditions they used with a pH electrode, and we demonstrated that net fluxes under the same conditions are comparable using both techniques. Wolosin and Ginsburg's (1975) permeability coefficient of $11 \times 10^{-4} \text{ cm s}^{-1}$ is slightly higher than the apparent permeability in our experiment ($P^{obs} = 6.3 \times 10^{-4} \text{ cm s}^{-1}$) (Table I), but their value was "corrected" for the unstirred layer thickness of their system from an estimated unstirred layer thickness of $80 \mu\text{m}$ and the following relation:

$$\frac{1}{P^{obs}} = \frac{1}{P^{ul}} + \frac{1}{P^m}, \quad (9)$$

so that their P^{obs} must have been $5.9 \times 10^{-4} \text{ cm s}^{-1}$. However, their correction is improperly made because Eq. 9 applies only to solutes with a single molecular species and does not take into account the gradients in $[A^-]$,

[HA], and $[H^+]$ that develop in the unstirred layers, or the facilitating effect of A^- on diffusion. The gradients that develop under these conditions were calculated as described in the Appendix and are shown graphically in Fig. 6. Almost the entire gradient in [HA] occurs across the unstirred layer with only a small gradient across the membrane. The membrane permeability calculated from the true transmembrane gradient in HA is $\sim 1 \times 10^{-2} \text{ cm s}^{-1}$, less than the $9.5 \times 10^{-2} \text{ cm s}^{-1}$ determined above from the symmetrical experiments. However, this calculated membrane permeability is very sensitive to small

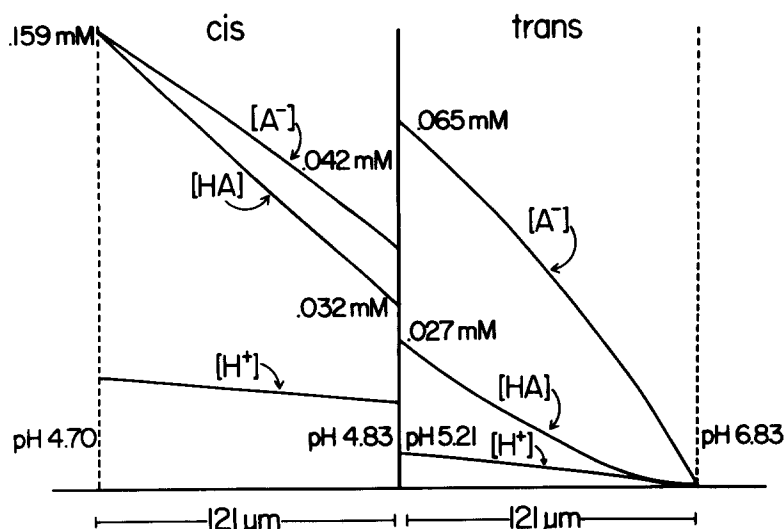


FIGURE 6. Concentration profiles of HA, A^- , and H^+ in the *cis* and *trans* unstirred layers that exist during butyric acid net flux experiments in the absence of buffer. The pH of the *cis* solution (100 mM NaCl, 0.16 mM total butyric acid) was 4.7 ($= pK_a$) and the pH of the *trans* solution (100 mM NaCl) was ~ 8 . The gradients were calculated as described in the Appendix from the unstirred layer thickness, the flux, diffusion coefficients, the dissociation constant, and the bulk concentrations. In the example, $J = 5.52 \times 10^{-11} \text{ mol cm}^{-2} \text{ s}^{-1}$, $D_{HA} = D_{A^-} = 8.67 \times 10^{-6} \text{ cm}^2 \text{ s}^{-1}$, $D_{H^+} = 9.31 \times 10^{-5} \text{ cm}^2 \text{ s}^{-1}$, and the activity coefficient for A^- and H^+ was 0.788.

changes in the flux or unstirred layer thickness. For example a 10% error in a measured parameter may be amplified to a 60% error in the calculated permeability. Thus, the accuracy of such calculations is poor.

From the above analysis it is clear that Wolosin and Ginsburg (1975) underestimated the membrane permeability coefficients for many weak acids because their fluxes were limited by events in the unstirred layers as shown in Fig. 6. This also implies that their proposed polymeric structure of egg phosphatidylcholine-decane membranes based on nonelectrolyte permeability coefficients must be reevaluated (see also Wolosin et al., 1978).

One question that has been raised (H. Ginsburg, personal communication) regarding the measurement of HA fluxes at high concentrations of A^- is the

possibility that A^- contributes to the flux by inserting itself in the membrane, then combining with an H^+ and crossing the membrane. This mechanism could increase the flux only if the entry step, i.e., movement of the solute (HA) from the aqueous to the membrane phase, is rate limiting for translocation. If insertion of A^- molecules and subsequent conversion to HA makes an important contribution to the flux of butyric acid, the flux should be a function of $[A^-]$. However, as shown in Figs. 2 and 3, the flux at high $[A^-]$ to $[HA]$ is independent of $[A^-]$. Furthermore, the value of P^m for butyric acid falls exactly on the regression line relating P^m to DK_p for a variety of nonelectrolytes, most of which are not weak acids (Orbach and Finkelstein, 1980).

Both methods, i.e., tracer fluxes at $pH \gg pK_a$ with symmetrical or well-buffered conditions or net fluxes measured by pH changes, can be used to measure weak acid and base permeabilities under certain circumstances. However, because of the relatively high permeabilities of most of these solutes, experiments must always be performed under several conditions to demonstrate that membrane permeabilities are not underestimated because of unstirred layer effects.

Not all weak acids and bases meet the criteria required for the approach developed in this paper. In particular for the uncouplers, which have highly permeant charged species, our approach will not circumvent the unstirred layer problem because the flux of the charged species will contribute to the total flux when $[A^-]/[HA]$ is very high. However, if the ionic species has a high permeability, electrical techniques can be used to estimate the permeabilities to both the ionic and nonionic forms (LeBlanc, 1971; McLaughlin and Dilger, 1980).

APPENDIX

Calculation of membrane permeability coefficients of weak acids and bases from net fluxes requires a means of determining the actual concentrations of the permeant species at the *cis* and *trans* membrane surfaces. A solution to this problem in the complete absence of buffer (a condition required for the *trans* solution when measuring fluxes with a pH electrode) is presented.

The concentrations of HA, A^- , and H^+ at the membrane surface can be determined by numerical integration of Fick's law of diffusion over the unstirred layer. The assumptions are (a) the flux is at or very near steady state, (b) the reacting species are in equilibrium with each other throughout the unstirred layer, i.e., the effective reaction relaxation distance is much smaller than the unstirred layer thickness (Gutknecht et al., 1972), and (c) no buffer is present. The parameters that must be known are the bulk solution concentrations, the dissociation constant (K), the net flux (J), the unstirred layer thickness, and the aqueous diffusion coefficients (D) of each species (or the unstirred layer permeability coefficient of each species).

The unstirred layer is divided into n planes parallel to the membrane of thickness x . By the law of conservation of mass and the constraint of steady state, the net flux through each plane is equal to the net flux across the

membrane and to the sum of the net fluxes of the individual species HA and A^- .

$$J = (J_{HA})_i + (J_{A^-})_i. \quad (1A)$$

Since HA is the only species crossing the membrane, the fluxes of H^+ and A^- through the unstirred layer must be equal and thus

$$J = (J_{HA})_i + (J_{H^+})_i. \quad (2A)$$

If each increment though the unstirred layer is sufficiently thin for the concentration gradients of each species to be linear, the fluxes may be written following Fick's First Law as:

$$(J_{HA})_i = \frac{D_{HA}}{x} ([HA]_i - [HA]_{i+1}); \quad (3A)$$

$$(J_{A^-})_i = \frac{D_{A^-}}{x} ([A^-]_i - [A^-]_{i+1}); \quad (4A)$$

$$(J_{H^+})_i = \frac{D_{H^+}}{x} ([H^+]_i - [H^+]_{i+1}). \quad (5A)$$

Since the relative concentrations of HA, A^- , and H^+ are related by the dissociation constant K , the concentration of one can be expressed in terms of the other two at all points through the unstirred layer if the rate of interconversion between the species is high relative to the rate of diffusion through the increment. For example:

$$[H^+] = \frac{K[HA]}{[A^-]}. \quad (6A)$$

The unknown variables in Eqs. 1A–6A are the three individual fluxes through each plane and the concentrations of the three molecular species at “i” and “i + 1.” Since the bulk concentrations are known, one may write the six equations above for the increment of unstirred layer adjacent to the bulk phase in terms of only six unknowns. Thus, these equations may be combined and solved. The bulk concentrations are represented by the index “i” in Eqs. 3A–5A for the *cis* unstirred layer and by “i + 1” for the *trans* unstirred layer. Our solution for the *cis* unstirred layer is outlined below. We combined Eqs. 1A–6A into two expressions in terms of $[HA]_{i+1}$ and $[A^-]_{i+1}$:

$$J = \frac{D_{HA}}{x} ([HA]_i - [HA]_{i+1}) + \frac{D_{A^-}}{x} ([A^-]_i - [A^-]_{i+1}); \quad (7A)$$

$$J = \frac{D_{HA}}{x} ([HA]_i - [HA]_{i+1}) + \frac{D_{H^+}K}{x} \left(\frac{[HA]_i}{[A^-]_i} - \frac{[HA]_{i+1}}{[A^-]_{i+1}} \right). \quad (8A)$$

The known terms of each equation are collected and set equal to single values, W and U , respectively:

$$W = J - \frac{D_{HA}}{x} [HA]_i - \frac{D_{A^-}}{x} [A^-]_i; \quad (9A)$$

$$U = J - \frac{D_{\text{HA}}}{x} [\text{HA}]_i - \frac{D_{\text{H}^+}K}{x} \frac{[\text{HA}]_i}{[\text{A}^-]_i}. \quad (10\text{A})$$

Substitution of W into Eq. 7A and rearranging gives an expression for $[\text{A}^-]_{i+1}$:

$$[\text{A}^-]_{i+1} = -\frac{x}{D_{\text{A}^-}} \left(W - \frac{D_{\text{HA}}}{x} [\text{HA}]_{i+1} \right). \quad (11\text{A})$$

Eq. 8A is rewritten using the value U and Eq. 11A and simplified by collecting the terms in $[\text{HA}]_{i+1}$ to give:

$$-\left(\frac{D_{\text{HA}}}{x}\right)^2 ([\text{HA}]_{i+1})^2 + \left(\frac{KD_{\text{A}^-} - D_{\text{H}^+}}{x^2} - \frac{D_{\text{HA}}}{x} (U + W)\right) [\text{HA}]_{i+1} - WU = 0. \quad (12\text{A})$$

Eq. 12A is in the form of a quadratic equation and its roots can be determined from $X = (-b \pm \sqrt{b^2 - 4ac})/2a$, where $a = -(D_{\text{HA}}/x)^2$, $b = [(KD_{\text{A}^-} - D_{\text{H}^+}/x^2) - (D_{\text{HA}}/x)(U + W)]$ and $c = -WU$.

$[\text{A}^-]_{i+1}$ is determined by Eq. 11A and $[\text{H}^+]_{i+1}$ is calculated from the equilibrium relation. This process is then repeated throughout the unstirred layer. A similar solution is obtained for the *trans* unstirred layer and the true membrane permeability is then calculated from the flux and the values of $[\text{HA}]$ at the membrane surface (see Eq. 4 in text).

Since the gradients in Eqs. 3A–5A are really activity gradients, appropriate activity coefficients are used with the assumption that these are constant throughout the unstirred layer, which is justified because the activity coefficients in our experiments are primarily a function of the supporting electrolyte concentration, i.e., ionic strength.

The solution presented above is useful for describing the concentration gradients throughout the unstirred layer but does not provide an accurate method for estimating membrane permeabilities when the unstirred layer effects are large. A 10% variation in any one of the measured parameters will cause a 40–60% change in the final calculated value for P^{m} when corrections are made for both unstirred layers. Thus, since most of these values cannot be measured to within a 10% accuracy, net flux experiments using a pH electrode are only useful for P^{m} determinations in situations when the unstirred layer correction is minimal, i.e., when the $\text{p}K_{\text{a}}$ is low or $P^{\text{m}} < P^{\text{ul}}$.

We thank Dr. S. A. Simon, Dr. D. W. Keifer, and B. Johnson for advice and critically reading the manuscript. We gratefully acknowledge correspondence with Dr. H. Ginsburg and discussions with Dr. A. Finkelstein.

This work was supported by National Institutes of Health grants GM 28844, HL 12157 and ES 02289.

Received for publication 11 August 1981 and in revised form 9 December 1981.

REFERENCES

- GUTKNECHT, J., L. J. BRUNER, and D. C. TOSTESON. 1972. The permeability of thin lipid membranes to bromide and bromine. *J. Gen. Physiol.* **59**:486-502.
- GUTKNECHT, J., and D. C. TOSTESON. 1973. Diffusion of weak acids across lipid bilayer membranes: effects of chemical reactions in the unstirred layers. *Science (Wash. D. C.)*. **182**:1258-1261.
- GUTKNECHT, J., and A. WALTER. 1981a. Transport of protons and hydrochloric acid through lipid bilayer membranes. *Biochim. Biophys. Acta.* **641**:183-188.
- GUTKNECHT, J., and A. WALTER. 1981b. Hydrofluoric and nitric acid transport through lipid bilayer membranes. *Biochim. Biophys. Acta.* **644**:153-156.
- GUTKNECHT, J., and A. WALTER. 1981c. Histamine, theophylline and tryptamine transport through lipid bilayer membranes. *Biochim. Biophys. Acta.* **649**:149-154.
- HODGKIN, A. L. 1951. The ionic basis of electrical activity in nerve and muscle. *Biol. Rev.* **26**:339-365.
- HOLZ, R., and A. FINKELSTEIN. 1970. The water and nonelectrolyte permeability induced in thin lipid membranes by the polyene antibiotics Nystatin and Amphotericin B. *J. Gen. Physiol.* **56**:125-145.
- LEBLANC, O. H., JR. 1971. The effect of uncouplers of oxidative phosphorylation on lipid bilayer membranes: carbonylcyanide-m-chlorophenylhydrazone. *J. Membr. Biol.* **4**:227-251.
- LYONS, P. A., and C. L. SANDQUIST. 1953. A study of the diffusion of *n*-butyl alcohol in water using the Gouy interference method. *J. Am. Chem. Soc.* **75**:3896-3899.
- McLAUGHLIN, S. G. A., and J. P. DILGER. 1980. Transport of protons across membranes by weak acids. *Physiol. Rev.* **60**:825-863.
- MUELLER, P., and D. O. RUDIN. 1969. Translocators in bimolecular lipid membranes: their role in dissipative and conservative bioenergy transductions. In *Current Topics in Bioenergetics*. Q. R. Sanadi, editor. Academic Press, Inc., New York. 157-249.
- ORBACH, E., and A. FINKELSTEIN. 1980. The nonelectrolyte permeability of planar lipid bilayer membranes. *J. Gen. Physiol.* **75**:427-436.
- PERRIN, D. D., and B. DEMPSEY. 1974. *Buffers for pH and Metal Ion Control*. Chapman and Hall, London. 176 pp.
- ROBINSON, R. A., and R. H. STOKES. 1959. *Electrolyte Solutions*. 2nd edition. Butterworths, London. 569 pp.
- WOLOSIN, J. M., and H. GINSBURG. 1975. The permeation of organic acids through lecithin bilayers: resemblance to diffusion in polymers. *Biochim. Biophys. Acta.* **389**:20-33.
- WOLOSIN, J. M., H. GINSBURG, W. R. LIEB, and W. D. STEIN. 1978. Diffusion within egg lecithin bilayers resembles that within soft polymers. *J. Gen. Physiol.* **71**:93-100.